European Community on Computational Methods in Applied Sciences

ECCOMAS Thematic Conference

COMPDYN 2019

7th International Conference on Computational Methods in Structural Dynamics and Earthquake Engineering

PROCEEDINGS

Volume I

M. Papadrakakis, M. Fragiadakis (Eds)

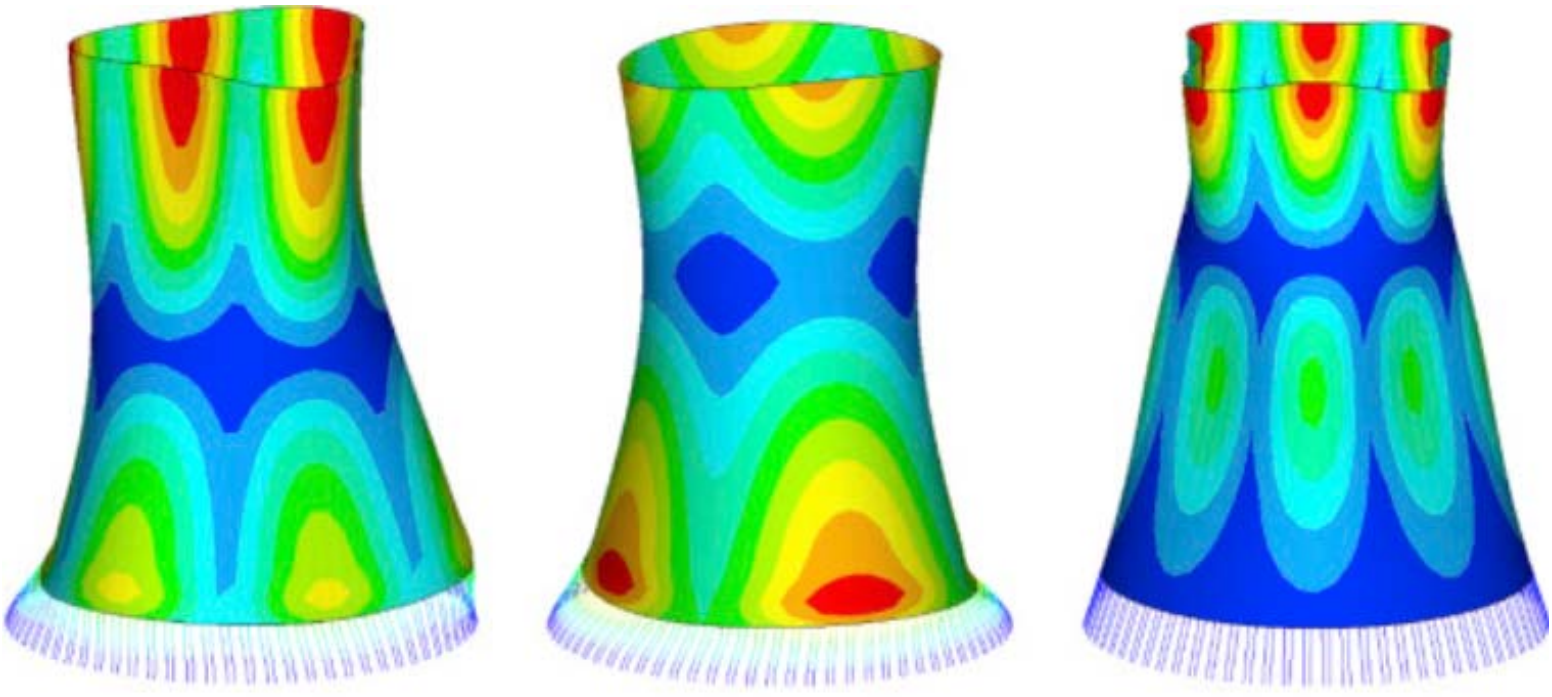

An IACM Special Interest Conference

COMPDYN 2019

Computational Methods in Structural Dynamics and Earthquake Engineering

Proceedings of the 7th International Conference on Computational
Methods in Structural Dynamics and Earthquake Engineering
Held in Crete, Greece
24-26 June 2019

Edited by:

M. Papadrakakis
National Technical University of Athens, Greece

M. Fragiadakis
National Technical University of Athens, Greece

A publication of:

Institute of Structural Analysis and Antiseismic Research
School of Civil Engineering
National Technical University of Athens (NTUA)
Greece

COMPDYN 2019
Computational Methods in Structural Dynamics and Earthquake Engineering
M. Papadrakakis, M. Fragiadakis (Eds)

First Edition, October 2019

ISBN (set): **978-618-82844-5-6**
ISBN (vol I): **978-618-82844-6-3**

PREFACE

This volume contains the full-length papers presented in the 7th International Conference on Computational Methods in Structural Dynamics and Earthquake Engineering (COMPDYN 2019) that was held on June 24-26, 2019 in Crete, Greece.

COMPDYN 2019 is one of the 32 Thematic Conferences of the European Community on Computational Methods in Applied Sciences (ECCOMAS) to be held in 2019 and is also a Special Interest Conference of the International Association for Computational Mechanics (IACM). The purpose of this Conference series is to bring together the scientific communities of Computational Mechanics, Structural Dynamics and Earthquake Engineering, to act as the forum for exchanging ideas in topics of mutual interests and to enhance the links between research groups with complementary activities. We believe that the communities of Structural Dynamics and Earthquake Engineering will benefit from their exposure to advanced computational methods and software tools which can highly assist in tackling complex problems in dynamic and seismic analysis and design, while also giving the opportunity to the Computational Mechanics community to be exposed to very important engineering problems of great social interest. The COMPDYN 2019 Conference is supported by the National Technical University of Athens (NTUA), the European Association for Structural Dynamics (EASD), the European Association for Earthquake Engineering (EAEE), the Greek Association for Computational Mechanics (GRACM).

The editors of this volume would like to thank all authors for their contributions. Special thanks go to the colleagues who contributed to the organization of the Minisymposia and to the reviewers who, with their work, contributed to the scientific quality of this e-book.

M. Papadrakakis
National Technical University of Athens, Greece

M. Fragiadakis
National Technical University of Athens, Greece

ACKNOWLEDGEMENTS

The conference organizers acknowledge the support towards the organization of the "7th International Conference on Computational Methods in Structural Dynamics and Earthquake Engineering", to the following organizations:

- European Community on Computational Methods in Applied Sciences (ECCOMAS)
- European Association for Structural Dynamics (EASD)
- European Association for Earthquake Engineering (EAEE)
- Greek Association for Computational Mechanics (GRACM)
- Hellenic Society for Earthquake Engineering (HSEE)
- School of Civil Engineering, National University of Athens (NTUA)
- Hellenic Republic-Region of Crete
- Municipality of Heraklion

Plenary Speakers and Invited Session Organizers

We would also like to thank the Plenary and Semi-Plenary Speakers and the Minisymposia Organizers for their help in the setting up of a high standard Scientific Programme.

Plenary Speakers: Michel Bruneau, Álvaro Cunha, Michael Fardis, Charbel Farhat, Christian Soize, Alexander Vakakis

Semi-Plenary Speakers: Christoph Adam, Gian Paolo Cimellaro, Eleni Chatzi, Geert Degrande, Boris Jeremic, Shinobu Yoshimura

MS Organizers: Günther Achs, Christoph Adam, Hamid Ahmadi, António Arêde, Rui Carneiro Barros, Michael Beer, Amadeo Benavent-Climent, Manuel Braz-Cesar, Alessandro Cabboi, Silvia Caprili, Claudia Casapulla, Serena Cattari, Nicola Cavalagli, Liborio Cavaleri, Jianbin Chen, Dimitris Chronopoulos, Alice Cicirello, Gian Paolo Cimellaro, Francesco Clementi, Marco Corradi, Flavia De Luca, Carlo Del Gaudio, Ciro Del Vecchio, Pedro Delgado, Raimundo Delgado, Raffaele Di Laora, Marco Di Ludovico, Luigi Di Sarno, Fabio Di Trapani, Francisco Alejandro Diaz de la O, Marco Domaneschi, Stefanos Dritsos, Hossein Ebrahimian, Antonio Formisano, Michalis Fragiadakis, Linda Giresini, Jose Gonzalez, Alexander Idesman, Alper Ilki, Maria Iovino, Fatemeh Jalayer, Hector Jensen, Andreas Kappos, Jin-Gyun Kim, Radek Kolman, Davide Lavorato, Guido Magenes, Charilaos Maniatakis, George Manos, Gabriele Milani, Stergios Mitoulis, Naoto Mitsume, Fabrizio Mollaioli, Paolo Morandi, Lukas Moschen, George Mylonakis, Jiri Naprstek, Ehsan Noroozinejad, Camillo Nuti, Roger Ohayon, Georgios S. Papavasileiou, K.C. Park, Vagelis Plevris, Nikos G. Pnevmatikos, Maria Polese, Laura Ragni, Andrei M. Reinhorn, Paolo Ricci, Hugo Rodrigues, Emmanouil Rovithis, Juan Chiachío Ruano, Manuel Chiachío Ruano, Walter Salvatore, Fabrizio Scozzese, Anastasios Sextos, Castorina Silva Vieira, Andrei L. Smirnov, Sergey Sorokin, Enrico Spacone, Daniele Spina, Constantine Spyrakos, Francesca Taddei, Anton Tkachuk, Petr Evgen'evich Tovstik, Savvas Triantafyllou, Yiannis Tsompanakis, Enrico Tubaldi, Marcos Valdebenito, Humberto Varum, Ioannis Vayas, Gerardo Mario Verderame, Stefania Viti, Shinobu Yoshimura

SUMMARY

VOLUME II

Minisymposia

VOLUME III

Regular Sessions

CONTENTS

VOLUME I

MS 3: EXPERIMENTAL MEASUREMENTS AND NUMERICAL SIMULATION ON PROBLEMS IN THE FIELD OF EARTHQUAKE ENGINEERING AND STRUCTURAL DYNAMICS

MS 6: SEISMIC SAFETY ASSESSMENT OF STRUCTURES

MS 7: RECENT ADVANCES IN THE DEVELOPMENT OF APPROXIMATE MATHEMATICAL TECHNIQUES FOR SOLVING COMPLEX SIMULATION-BASED PROBLEMS INVOLVING UNCERTAINTY

MS 8: RIGID BLOCK MODELING APPROACHES FOR STATIC AND DYNAMIC ANALYSIS OF MASONRY STRUCTURES IN SEISMIC AREAS

MS 9: NON-LINEAR DYNAMICS, WAVE PROPAGATION AND CONTACT-IMPACT PROBLEMS

MS 10: PROGRESS AND CHALLENGES IN RAIL TRACK DYNAMICS

MS 11: POST-EARTHQUAKE ASSESSMENT FOR BUILDINGS AND INFRASTRUCTURES AND REPARABILITY DECISIONS

MS 12: REPAIR AND RETROFIT OF STRUCTURES

MS 13: RECENT NUMERICAL MODELLING TRENDS FOR THE PRESERVATION OF HISTORICAL MASONRIES IN SEISMIC AREAS

MS 15: ADVANCES IN NUMERICAL METHODS FOR LINEAR AND NON-LINEAR DYNAMICS AND WAVE PROPAGATION

MS 17: SEISMIC RISK ASSESSMENT OF BUILDING PORTFOLIOS

MS 18: POTENTIAL OF VIBRATIONS MONITORING FOR IMPROVING THE RELIABILITY OF BUILDINGS SEISMIC ASSESSMENT

VOLUME II

MS 24: INFLUENCE OF INFILL MASONRY WALLS IN THE RESPONSE AND SAFETY OF BUILDINGS

MS 25: SPECIAL DESIGN AND ANALYSIS OF STRUCTURES

MS 26: RECENT ADVANCES ON ENERGY-BASED SEISMIC DESIGN

MS 27: ADVANCES IN MODEL REDUCTION TECHNIQUES IN COMPUTATIONAL STRUCTURAL DYNAMICS

MS 28: NEW ADVANCES IN COMPUTATIONAL MODELLING AND EXPERIMENTAL TESTING OF INFILLED FRAMES

MS 29: AFTERSHOCK RISK ASSESSMENT: STATE OF THE ART AND FUTURE CHALLENGES

MS 30: STRUCTURAL PERFORMANCE OF NEW AND EXISTING REINFORCED CONCRETE BUILDINGS IN SEISMIC AREAS: NUMERICAL AND EXPERIMENTAL APPROACHES FOR MODELLING

MS 31: MUSEUMS' COLLECTIONS AND SEISMIC PREVENTION: RESEARCH DEVELOPMENTS AND CASE-STUDIES

MS 33: SEISMIC RESILIENCE OF MUSEUM CONTENTS

MS 35: DAMAGE MODELLING, DETECTION AND IDENTIFICATION IN COMPOSITE STRUCTURES

MS 36: SEISMIC ASSESSMENT OF EXISTING STRUCTURES BEFORE AND AFTER STRENGTHENING

MS 38: RELIABILITY ASSESSMENT AND DESIGN OF STRUCTURES EQUIPPED WITH ISOLATION AND DISSIPATION DEVICES

MS 39: PERIODICITY EFFECTS IN VIBRO-ACOUSTICS

MS 40: DYNAMICS OF BUILDINGS AND BRIDGES AND CONTROL STRATEGIES WITHIN STRUCTURAL ENGINEERING

MS 41: THIN-WALLED STRUCTURES, STRENGTH, VIBRATION AND STABILITY

MS 42: NOVEL METHODS FOR SEISMIC DESIGN AND INTERVENTION OF CONVENTIONAL AND INTEGRAL BRIDGES

MS 44: DYNAMIC BEHAVIOUR OF JOINTS AND JOINTED STRUCTURES: MODELLING AND EXPERIMENTS

MS 45: ADVANCES ON EXPERIMENTAL AND COMPUTATIONAL SEISMIC ASSESSMENT AND RETROFIT OF MASONRY STRUCTURES

VOLUME III

Regular Sessions

RS 2: ALGORITHMS FOR STRUCTURAL HEALTH MONITORING

RS 3: CONSTITUTIVE MODELLING UNDER EARTHQUAKE LOADING

RS 4: DYNAMICS OF CONCRETE STRUCTURES

RS 5: DYNAMICS OF COUPLED PROBLEMS

RS 7: DYNAMICS OF STEEL STRUCTURES

RS 8: GEOTECHNICAL EARTHQUAKE ENGINEERING

RS 9: IMPACT DYNAMICS

RS 10: INVERSE PROBLEMS IN STRUCTURAL DYNAMICS

RS 12: NONLINEAR DYNAMICS

RS 13: NUMERICAL SIMULATION METHODS FOR DYNAMIC PROBLEMS

RS 14: OPTIMUM DESIGN AND CONTROL IN STRUCTURAL DYNAMICS AND EARTHQUAKE ENGINEERING

RS 16: PERFORMANCE-BASED EARTHQUAKE ENGINEERING

RS 20: SEISMIC RISK AND RELIABILITY ANALYSIS

RS 26: STEEL STRUCTURES

RS 27: STOCHASTIC DYNAMICS

RS 29: WAVE PROPAGATION

COMPDYN 2019
7th ECCOMAS Thematic Conference on
Computational Methods in Structural Dynamics and Earthquake Engineering
M. Papadrakakis, M. Fragiadakis (eds.)
Crete, Greece, 24–26 June 2019

EFFECTS OF MODELING ASSUMPTIONS ON THE EVALUATION OF THE LOCAL SEISMIC RESPONSE FOR RC PRECAST INDUSTRIAL BUILDINGS

M.E. Bressanelli[1], A. Belleri[1], P. Riva[1], G. Magliulo[2], D. Bellotti[3], and B. Dal Lago[4]

[1] University of Bergamo, Department of Engineering and Applied Sciences.
Dalmine, Italy. {michele.bressanelli, andrea.belleri, paolo.riva}@unibg.it

[2] University of Naples Federico II, Department of Structural Engineering
Napoli, Italy. gmagliul@unina.it

[3] European Centre for Training and Research in Earthquake Engineering
Pavia, Italy. Davide.bellotti@eucentre.it

[4] Politecnico di Milano, Department of Civil and Environmental Engineering
Milano, Italy. brunoalberto.dallago@polimi.it

Abstract

The present research is aimed at evaluating the influence of different modelling assumptions, such as crane-load and beam-column connections, on the local seismic response of precast RC buildings. The considered case study is a one-story industrial building designed in accordance with the Italian building code NTC 2008. Typical pinned beam-column connections are investigated. They are made by dowels protruding from the column inserted into holes in the beams, which are subsequently grouted. This technique ensures stability during the construction process and allows the horizontal seismic load transfer from the beam to the column. Different structural layouts have been modeled considering various types of beam-column joint models, namely a perfect hinge, an elastic hinge and a non-linear spring with a degrading hysteretic force-displacement model; the last model reproduces the results of recent experimental campaigns. Non-linear dynamic time history analyses allow to evaluate displacements, drifts, deformations and ultimate curvatures. The results are analyzed in terms of both global quantities, i.e. roof maximum displacements and rotation at the base of the columns, and local quantities, i.e. force or displacement demand at the beam-column connections, for the various implemented models. Depending on the considered model, it is observed that the effects of higher vibrating modes may increase the load in the connections.

Keywords: Higher mode vibration, Crane load, Dowel connection, Demand-capacity ratio, Simplified model, Precast industrial building.

1 INTRODUCTION

Precast structures are recognized as being able to ensure many benefits as the ability to cover large surfaces, the high-quality control of materials and elements and the reduced construction time compared to traditional structures. For these reasons, these structures have been commonly adopted in industrial building.

Precast structures are typically characterized by a simple structural layout with cantilever columns pin-connected to pre-stressed beams supporting roof elements. Generally, the columns are either placed inside pocket footings or connected to the foundation by means of mechanical devices or grouted sleeves [1],[2],[3],[4]. In the past, beams were either simply supported on the columns, or connected to them through dowels. The contact surface was typically equipped with a neoprene pad to spread the load over the support. The simple-support connections relying solely on friction for the horizontal load transfer are typical of existing precast industrial structures designed only for vertical loads, in zones that have been classified seismically hazardous only in the last decades. In the case of dowel connections, one or more steel dowels are embedded in the column and inserted in a beam hole, filled with mortar.

Recent earthquakes in Italy highlighted many vulnerabilities of existing industrial precast structures [5],[6],[7],[8]. The main collapses experienced by these structures are related to: fall of roof elements caused by high relative displacement and loss of support, loss of support in the beam-to-column connections, rupture of the mechanical connections and consequent fall of cladding panels [9],[10],[11]. The collapse of the reinforced concrete forks at the top of the columns and collapse of the columns were also observed. The frame connections are crucial in precast industrial buildings, given that they may inhibit the exploitation of strength and ductility reserves in precast elements. The lack of connections between roof elements leads to a higher global flexibility of the roof system with a non-rigid diaphragm effect which may activate higher modes [12],[13]. This can lead to the development of mechanisms due to relative movements between structural elements. Furthermore, given the different distribution of the participating mass and the stiffening effect provided by cladding panels, the flexibility of the floor causes differences in the seismic response between the internal and external frames. In this way, the main damage is mainly linked with the loss of support and fall of the horizontal structural elements (roof elements and beams) due to the lack or reduced ability of the mechanical connections to achieve a proper restraint. Several studies have analyzed the performance of existing precast structures and how to make them earthquake proof [14],[15], [16],[17],[18],[19],[20],[21].

The research presented herein is aimed at evaluating the failure probability of new precast structures designed according to the current Italian seismic regulations as part of a national project financed by the Italian Civil Protection focused on the assessment of new and existing buildings [22],[23],[24],[25],[26],[27]. The influence of different modelling strategies on the failure rate are analyzed taking as reference a typical precast building.

2 CASE STUDY STRUCTURE

The reference structure is a single-story 4-bay precast reinforced concrete (RC) industrial building considered built at L'Aquila (Italy) with span length along the transverse x-direction equal to 15 m and 6 m along the longitudinal y-direction (Figure 1). The structural elements are designed and verified [28] according to the Italian building code [29] and commentary [30]. For further structural verifications, not available or not fully addressed in the Italian building code, Eurocode 2 CEN 2004, Eurocode 3 CEN 2005, CNR 10018/99 and CNR 10025/98 provisions were considered [31],[32],[33],[34].

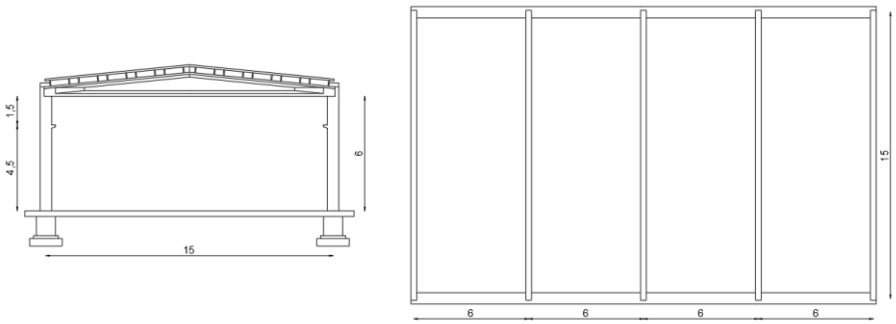

Figure 1: Schematic transverse frame (left) and plan view (right).

The case study structure consists of precast square columns fixed at the base with isolated socket foundations, connected in both directions by RC beams on grade. All the precast elements are made of C45/55 concrete and B450C steel. The columns, with a longitudinal reinforcement ratio equal to 2.5%, are connected, by means of dowel connection, to the main precast prestressed beams. The dowel connection is considered effective only in the transverse direction, due to the presence of a RC fork at the top of the column inhibiting the beam movements in the longitudinal direction. The height of the column is 6 m, with a corbel at 4.5 m supporting the overhead crane. The beams are double-tapered with 10% slope and are characterized by a variable I-shaped cross-section. The longitudinal girder beams have a rectangular cross section (0.3 m x 0.5 m) and provide a support to the cladding system. The roof is made by precast TT-shaped elements above which a cast in place concrete slab (C25/30, 5 cm thickness), provides a rigid diaphragm.

The cladding system consists of vertical precast panels, with specific weight of 4 kN/m^2, connected to the longitudinal girder beams. Considering the industrial use for the building, the presence of a crane is taken into account: precast corbels in the internal side of the columns support crane runway beams, HE400A, on which the crane is supported. For this structural typology, the structural behavior factor q is equal to 2.5 for low ductility class. Lumped masses are placed in the model: m_C is equal to 2.13 kN/g at each corbel position (corresponding to an equal distribution among the columns of the crane mass and 80% of the crane payload, according to the Italian building code for structures of category D [29]), m_T at the top of each central column is equal to 37.90 kN/g in the horizontal directions and 28.85 kN/g in the vertical direction, while at each end column m_T is equal to 37.40 kN/g in the horizontal directions and 16.50 kN/g in the vertical direction. Where m_T represents the mass of the roof system and cladding panels, while m_C indicates the crane mass. The differences of the values of m_T in the vertical directions are related to the weight of the cladding system which is not participating in the vertical excitation.

3 MODELING AND ANALYSIS

In order to perform non-linear dynamic analyses, numerical models are created in the OpenSees software [35]. Six simplified modelling assumptions (Figure 2) are considered to evaluate the influence of modeling choices on the results.

The first model (model A) is the reference model. The columns are fixed at the base. The main beams and the girders are modeled with elastic elements; a constant cross section is assigned to the main beams as the mean value of the variable height and width. Perfect hinge constraints are considered between girder beams and columns and between the main beams and columns. The cladding panels are not considered in the model in terms of lateral stiffness, but only in terms of masses and loads applied to the main structure. This reflects the hypothe-

sis that the cladding panels are connected to the structure with isostatic pendulum connection arrangement [36]. The non-linear behavior of the structural elements is modeled considering a lumped plasticity approach with plastic hinges at the column bases including plastic deformation and elastic column elements. The curvature and the yielding moment of the columns are obtained from a fiber analysis of the column cross-section. The plastic hinge at the base of the columns is modelled with a zero-length element considering the Modified Ibarra-Medina-Krawinkler Deterioration Model with peak-oriented hysteretic response [37]: effective yielding moment M_y equal to 1256 kNm, effective stiffness K_e equal to $4.37 \cdot 10^4$ kN/m and cyclic deterioration parameter λ equal to 2.734. The second model (model B) differs from model A only for the overhead crane mass m_C with no account of the pay load [38], therefore m'_C is equal to 1.329 kN/g. The third model (model C) is similar to model A, but the main beam-to-column connections are at their real position, i.e. at the interface between the beam and the column and not at the beam center-line. The forth model, model D, is equal to model C, with reduced crane loads (equal to model B). Two additional models, model E and model F (Figure 3), are defined to analyze effects of modelling assumptions of the dowel connection between the main beams and the columns. Such connections are modeled using a non-linear spring with a degrading hysteretic model in terms of force and displacement, i.e. Modified Ibarra-Medina-Krawinkler deterioration model. To specifically evaluate the effects of the higher modes of vibration, the two models have different Rayleigh damping coefficients α and β. In model F, all the relevant masses are concentrated in the center of the roof diaphragm. Such mass is equal to 425 kN/g in the two horizontal directions and 287 kN/g in the vertical direction.

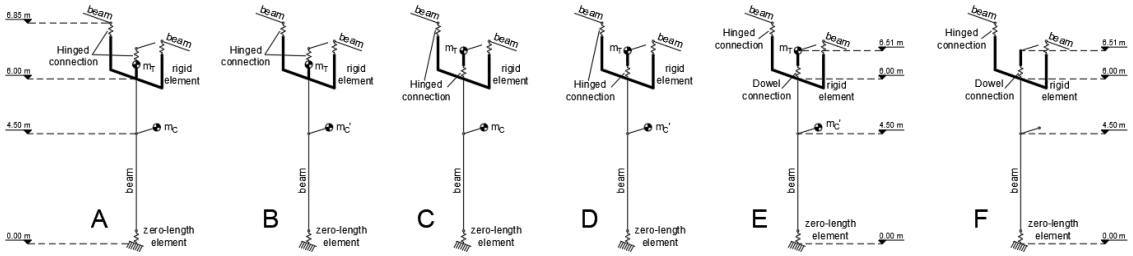

Figure 2: Main simplified models considered.

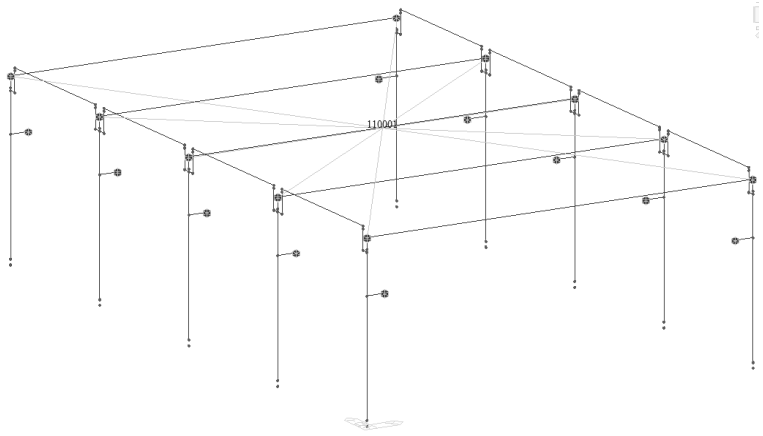

Figure 3: Schematic view of model E.
Note: the circles indicate the position of the masses in the modelled structure with OpenSees.
The number 110001 in the center indicates the degree of constraint of the diaphragm floor, i.e. blocked relative displacements in the horizontal directions.

3.1 Beam-to-column dowel connection

The connections between the principal beams and the columns are made by steel dowels protruding from the column, inserted into holes in the beams and subsequently grouted. The connections are designed with a shear action resulting from capacity design and a shear strength resulting from the following formulation [39],[40],[41].

$$V_{Rm} = n \cdot \alpha \cdot d_b^2 \cdot \sqrt{f_{ym} \cdot f_{cm}} \tag{1}$$

In this formulation n represents the number of dowels, d_b the dowel diameter, f_{ym} the mean value of yielding of the dowels, f_{cm} is the concrete mean compression strength and α is a reduction factor [42],[43],[44]. For this case, f_{ym} is equal to 816 MPa, f_{cm} is equal to 60 MPa. The connections have been designed with a coefficient α equal to 1,6 according to [34] and have been checked against failure with a more recent and conservative formulation provided in the design guidelines of the Safecast project [45] with a coefficient α equal to 0.9.

The design process led to 2 steel dowels with 24 mm diameter for each joint.

The stiffness of beam-to-column dowel's connection is calculated with the following formulation derived by Ferreira [46]:

$$\lambda = \frac{1}{K} = \left[\frac{n \cdot E_s \cdot \pi \cdot d_b^4}{64} \cdot \left(\frac{t_n^3}{12} + \frac{1}{3.5 \cdot \alpha_g^3} + \frac{1}{3.5 \cdot \alpha_{cls}^3} \right)^{-1} + \frac{G_n \cdot (b \cdot h)_n}{t_n} \right]^{-1} \tag{2}$$

Where subscript n indicates neoprene and g indicates grout. Yielding displacement is computed according to:

$$d_y = \lambda \cdot F_y \tag{3}$$

Where F_y is computed according to (1). The yield displacement of the connection for this case study is equal to 2.8 mm.

In model E, as a result of the cyclic tests of Kremmyda [47], the capping displacement is conservatively assumed equal to the diameter of the dowel, i.e. 24 mm, while the ultimate displacement capacity equal to twice the diameter of the dowel (Figure 4). In model F the value of the capping displacement is equal to half the diameter of dowel, i.e. 12 mm, and the ultimate displacement is equal of 1.5 times, i.e. 36 mm. The yield displacement is the same.

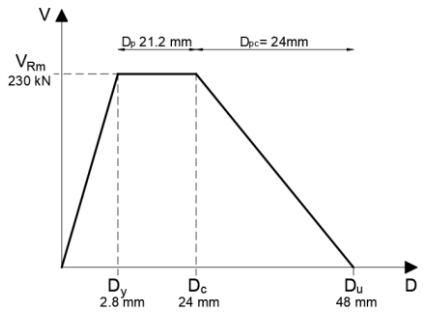

Figure 4: Beam-to-column dowel's connection in model E.

3.2 Seismic input

Non-linear dynamic analyses, i.e. time history analyses, are performed for ten different intensity motion (IM), with increasing intensity, from PGA equal to 0.011 g to 1.077 g. Each IM has twenty records in both horizontal directions and it corresponds to a defined return pe-

riod T_r (Table 1). The records were selected according to the conditional mean spectrum approach [48]. The value of the reference period was selected to be appropriate for the fundamental period of the considered structure (2.0 s).

Table 1: Intensity motion in the analyses.

Intensity motion	T_r [years]	PGA [g]
1	10	0.011
2	50	0.026
3	100	0.049
4	250	0.080
5	500	0.124
6	1000	0.184
7	2500	0.27
8	5000	0.379
9	10000	0.572
10	100000	1.077

4 DISCUSSION OF THE RESULTS

The results are analyzed in terms of both global response (Figure 5), i.e. roof maximum displacement and rotation at the base of the columns, and local response (Figure 6), i.e. force and displacement demand in the beam-to-column connections. For the global response, the maximum displacement capacity is that corresponding to a 50% reduction of the shear at the base of the column, obtained from a non-linear static analysis. While the maximum rotation capacity at the column base is that corresponding to a post-peak reduction of 50% of the bending moment. To evaluate the differences among the various models, the results are firstly presented for one ground motion of IM 9, with PGA equal to 0.572 g. For the local response in terms of shear force in the dowel connection, reference is made to its maximum shear capacity. For the evaluation in terms of relative displacement, the beam-to-column connection capacity is defined by the displacement at a post-peak reduction of 50% of the maximum shear in model E, while, in model F, this capacity is defined at a post-peak reduction of 20%.

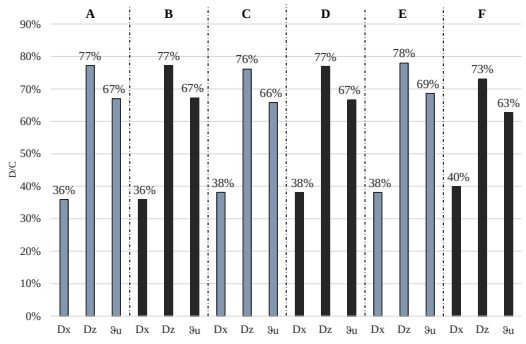

Figure 5: Demand/Capacity (D/C) global evaluation.

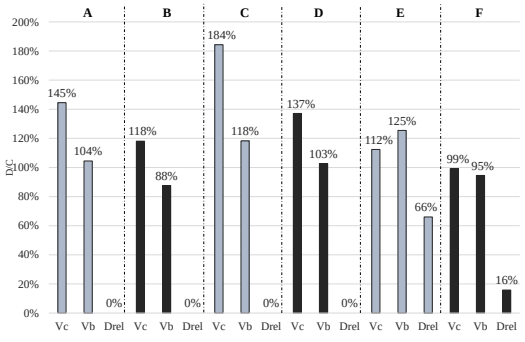

Figure 6: Demand/Capacity (D/C) local evaluation.

Comparing the models, in particular A with C and B with D, the lowering of the vertical position of the zero-length element associated with the hinge connection leads to a decrease of the shear span in the column with a consequent increase of the shear demand. Table 2 and Table 3 compare the main results between the models. It is possible to state that the global re-

sponse is not influenced by the type of modeling conducted; indeed, the global response in terms of displacement at the roof level does not show any difference between the models because the displacement is governed by the first mode of vibration. Instead, important differences are present in the local response.

Table 2: D/C global evaluation for GM1 with IM9.

Model	D_x: f(50%·$V_{pushover}$)	D_y: f(50%·$V_{pushover}$)	ϑ: f(50%·V_{max})
A	36%	77%	67%
E	38%	78%	69%
F	40%	73%	63%

Table 3: D/C local evaluation for GM1 with IM9.

Model	$V_{connection}$	$V_{base\ column}$	D_{rel}(α%·Fmax)
A	145%	104%	Hinge model
E	112%	125%	66% (for α=50)
F	99%	95%	16% (for α=80)

It is interesting to note that in model A, the higher value of shear in the beam-to-column connection is caused by the higher modes of vibration of the columns; if we remove the masses on the columns (i.e. the mass of the crane load) this effect vanishes. Similarly, the shear at the base of the column in model E is higher than in model A for the effect of higher modes of vibration associated with a low damping ratio. On the other end, lumping all the masses in only one point in the roof center, as in model F, leads to lower shear values in the beam-to-column connections.

The following figures show the contribution of the higher modes of vibration: the 1st and 3rd modes are associated with global displacement in the horizontal directions, the 2nd mode is associated with torsional motion of the structure, while the 4th mode is responsible of increasing loads in the connection particularly sensitive to the value of Rayleigh damping ratio.

To investigate the effects of higher modes of vibration, the difference between Rayleigh damping proportional to the mass and stiffness matrices and to the sole mass matrix is analyzed. The damping ratio for the nth mode of the system in the case of Rayleigh damping is:

$$\xi_n = \frac{1}{2} \cdot \left(\frac{\alpha}{w_n} + \beta \cdot w_n \right) \tag{5}$$

with α and β defined as:

$$\alpha = \xi \cdot \frac{2 \cdot w_1 \cdot w_3}{w_1 + w_3}; \ \beta = \frac{2 \cdot \xi}{w_1 + w_3} \tag{6) (7}$$

Where w_1 and w_3 are the circular frequencies of the elastic system relative to the first and the third vibration modes, respectively. The damping curve is defined as a function of the period of the structure T and relative damping ξ (Figure 11).

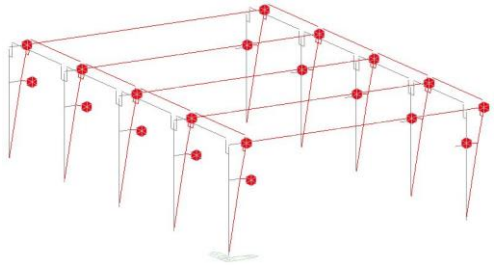

Figure 7: 1st mode of vibration of model A.

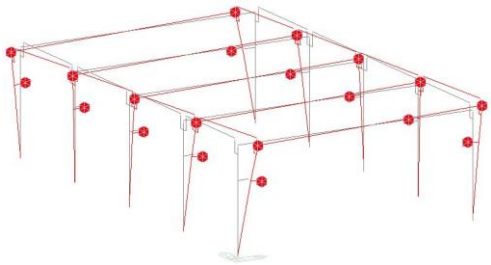

Figure 8: 2nd mode of vibration of model A.

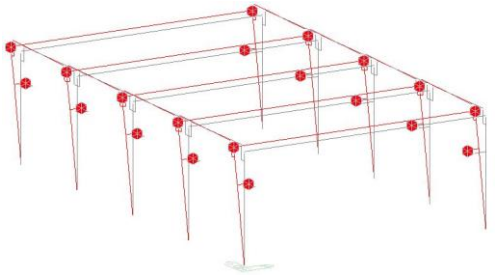

Figure 9: 3rd mode of vibration of model A.

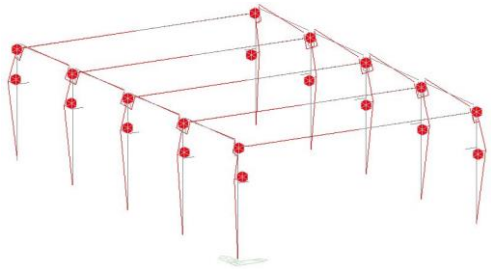

Figure 10: 4th mode of vibration of model A.

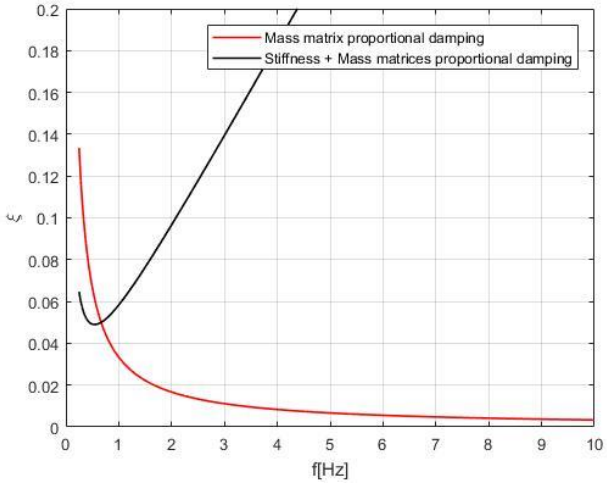

Figure 11: Rayleigh damping.

In the case of mass matrix proportional damping, for the first period, approximately equal to 1.5 s (0.67 Hz), the relative damping is 5% (Figure 11). For higher vibration modes, for example the 4th (14.72 Hz), the relative damping is very low (under 5‰). Therefore, considering the crane mass at the column corbel, a portion of the participating mass is in correspondence to higher vibration modes and it is subjected to very low damping values. In addition, as in model A, the low rotational stiffness at the column base after the development of a plastic hinge compared to the high axial stiffness of the beam leads to an uneven shear distribution with higher values in the connection (Figure 12a). The increase of the shear in the connection leads to evaluations in terms of shear worse than in terms of relative displacement. In the case of hysteretic beam-to-column connections, once the connection yield, the shear distribution along the column corresponds to Figure 12b.

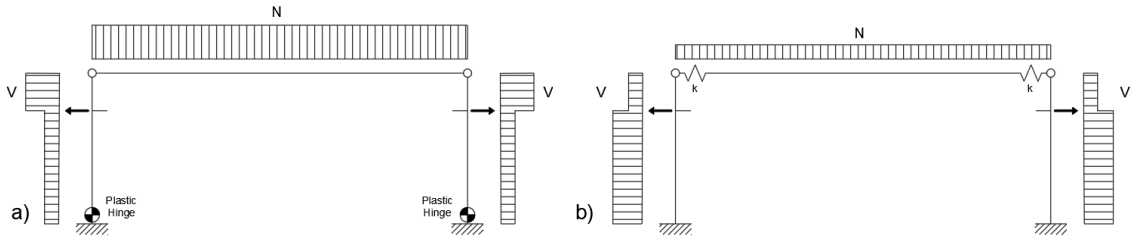

Figure 12. Distribution of internal actions after the development of the plastic hinges at the base of the columns as in model A (left side) and in the case of beam-to-column connections as in model F (right side).

The previous assessment in terms of global and local demand/capacity for one ground motion is now extended to all ground motions and all IM. Figure 13 shows the results in terms of demand-capacity ratio (D/C) for model F; for each intensity motion, the results of the local evaluation in terms of relative displacements of the beam-to-column connection are represented in gray, while the global evaluation in terms of maximum displacement at the top of the column is represented in black. The results show collapses of some beam-to-column connections for PGA equal or larger than 0.27 g. When the seismic intensity increases, there are several collapses of the connections. The following figures (Figures 14-17) show the cumulative distribution of the damage as function of IM. IM10, with PGA equal to 1.077 g, causes the collapse of all the connections of this precast industrial building.

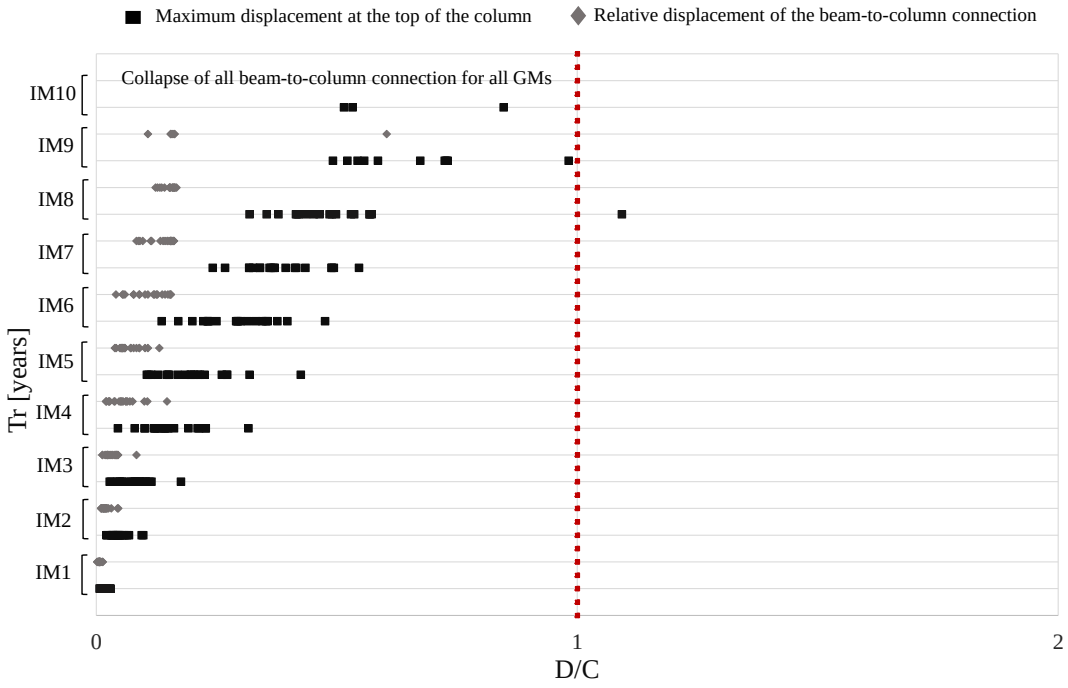

Figure 13: Demand/Capacity (D/C) for model F.

For low IM, both global and local assessments show a gradual increase in damage (Figure 13). The low dispersion of D/C results highlights a good accuracy of the results. While, for high IM, i.e. for PGA values above 0.27 g, the results in terms of local assessments are more scattered. For example, considering the IM9, the local evaluation shows results ranging from a linear behavior of the beam-to-column connections to their failure.

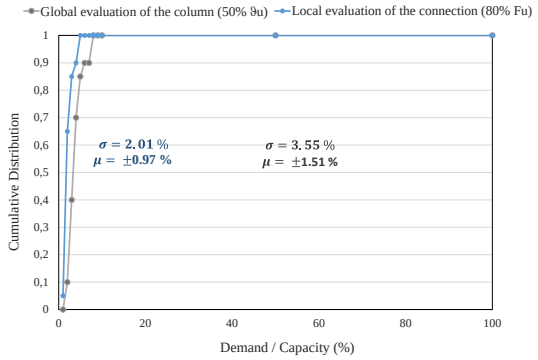

Figure 14: Evaluation of the IM2 of Model F.

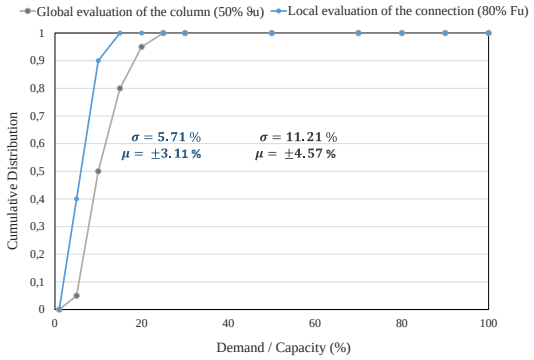

Figure 15: Evaluation of the IM4 of Model F.

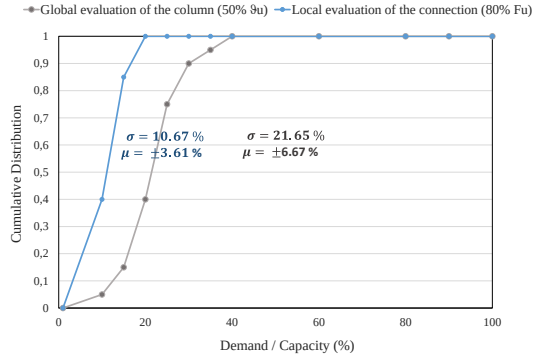

Figure 16: Evaluation of the IM6 of Model F.

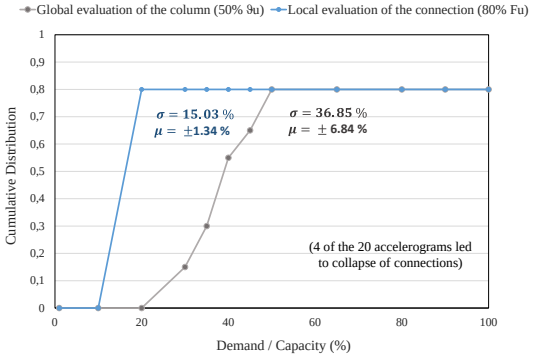

Figure 17: Evaluation of the IM8 of Model F.

5 CONCLUSIONS

The present paper analyzed the influence of finite element modelling in the evaluation of the collapse rate of precast industrial buildings, referring in particular to beam-to-column connections. A single-story precast industrial building was selected as reference structure and modelled in OpenSees with different assumptions, such as the distribution of the overhead crane mass (i.e. equally distributed on each column corbel and with or without accounting for the payload) and the beam-to-column connections (i.e. hinged or dowel connection), for a total of six models. Non-linear dynamic analyses with increasing intensity were carried out (PGA ranging from 0.011 g to 1.077 g). The results showed that in model A (i.e. the model with plastic hinges at the base of the columns, crane mass at corbel position and beam-to-column hinged connection at the top of the column) the effect of higher modes of vibration causes a higher value of shear in the connections. Removing the masses of the crane load makes this effect vanishing. In model E, where the dowel connections are explicitly modelled in terms of force-displacement hysteretic curve, the shear at the base of the columns is higher than in the model A, when mass proportional Rayleigh damping is selected. Besides, the lowering of the vertical position of the beam-to-column connection, for example in model C and D, leads to an increase of the shear in the connections due to the decrease of the shear span.

For low levels of intensity motions, both global and local assessments show a gradual increase in damage; while, for higher values, the results in terms of local response are more scattered.

The models of the precast building showed many collapses of beam-to-column connections for medium and high intensity motions. In these numerical simulations, the collapse of the

connections is considered as a global collapse of the structure. The analyses on the model F, i.e. the most representative model for this precast structure, show collapses of several connections for PGA equal or higher than 0.27 g. For PGA greater than 1.077 g all the connections fail. Despite capacity design was used for these connections, this result reflects a design formulation taken from an aged Italian co-normative document and a stricter check formulation taken from a more recent Communitary design guideline report.

AKNOWLEDGEMENTS

The study presented in this article was developed within the activities of the ReLUIS-DPC 2014-2018 research program; however, opinions and conclusions do not necessarily reflect those of the funding entity.

REFERENCES

[1] A. Belleri, P. Riva, Seismic performance and retrofit of precast concrete grouted sleeve connections. *PCI Journal*, 57(1), 97–109, 2012.

[2] G. Metelli, C. Beschi, P. Riva, Cyclic behaviour of a column to foundation joint for concrete precast structures. *European Journal of Environmental and Civil Engineering*, 15(9), 1297–1318, 2011.

[3] Z.B. Haber, M.S. Saiidi, D.H. Sanders, Seismic performance of precast columns with mechanically spliced column-footing connections. *ACI Structural Journal*, 111(3), 639–650, 2014.

[4] B. Dal Lago, G. Toniolo, M. Lamperti Tornaghi, Influence of different mechanical column-foundation connection devices on the seismic behaviour of precast structures, *Bulletin of Earthquake Engineering*, 14(12), 3485-3508, 2016.

[5] A. Belleri, E. Brunesi, R. Nascimbene, M. Pagani, P. Riva, Seismic performance of precast industrial facilities following major earthquakes in the Italian territory. *Journal of Performance of Constructed Facilities*, 29(5), 2015.

[6] A. Belleri, M. Torquati, P. Riva, R. Nascimbene, Vulnerability assessment and retrofit solutions of precast industrial structures. *Earthquakes and Structures*, 8(3), 801–820, 2015.

[7] G. Magliulo, M. Ercolino, C. Petrone, O. Coppola, G. Manfredi, The Emilia earthquake: seismic performance of precast reinforced concrete buildings. *Earthquake Spectra*, 30(2), 891–912, 2014.

[8] D.A. Bournas, P. Negro, F.F. Taucer, Performance of industrial buildings during the Emilia earthquakes in Northern Italy and recommendations for their strengthening. *Bulletin of Earthquake Engineering*, 12(5), 2383–2404, 2014.

[9] A. Belleri, F. Cornali, C. Passoni, A. Marini, P. Riva, Evaluation of out-of-plane seismic performance of column-to-column precast concrete cladding panels in one-storey industrial buildings. *Earthquake Engineering and Structural Dynamics*, 47, 397-417, 2017.

[10] A. Belleri, M. Torquati, A. Marini, P. Riva, Horizontal cladding panels: in-plane seismic performance in precast concrete buildings. *Bulletin of Earthquake Engineering*, 14, 1103-1129, 2016.

[11] M. Ercolino, G. Magliulo, G. Manfredi, Failure of a precast RC building due to Emilia-Romagna earthquakes. *Engineering Structures*, 118, 262-273, 2016.

[12] B. Dal Lago, L. Ferrara, Efficacy of roof-to-beam mechanical connections on the diaphragm behaviour of precast decks with spaced roof elements. *Engineering Structures*, 176, 681-696, 2018.

[13] B. Dal Lago, S. Bianchi, F. Biondini, Diaphragm effectiveness of precast concrete structures with cladding panels under seismic action. *Bulletin of Earthquake Engineering*, 17(1), 473-495, 2019.

[14] A. Belleri, M. Torquati, P. Riva, Seismic performance of ductile connections between precast beams and roof elements. *Magazine of Concrete Research*, 66(11), 553–562, 2014.

[15] M. Torquati, A. Belleri, P. Riva, Displacement-Based Seismic Assessment for Precast Concrete Frames with Non-Emulative Connections. *Journal of Earthquake Engineering*, 2018.

[16] A. Belleri, A. Marini, P. Riva, R. Nascimbene, Dissipating and re-centring devices for portal-frame precast structures. *Engineering Structures*, 150, 736-745, 2017.

[17] A. Belleri, Displacement based design for precast concrete frames with not-emulative connections. *Engineering Structures*, 141, 228-240, 2017.

[18] G. Magliulo, M. Cimmino, M. Ercolino, G. Manfredi, Cyclic shear tests on RC precast beam-to-column connections retrofitted with a three-hinged steel device. *Bulletin of Earthquake Engineering*, 15(9), 3797-3817, 2017.

[19] E. Brunesi, R. Nascimbene, D. Bolognini, D. Bellotti, Experimental investigation of the cyclic response of reinforced precast concrete framed structures. *PCI Journal* 60(2), 57-79, 2015.

[20] A. Titi, F. Biondini, G. Toniolo, Seismic assessment of existing precast structures with dry-friction beam-to-column joints. *Bulletin of Earthquake Engineering*, 16(5), 2067-2086, 2018.

[21] B. Dal Lago, P. Negro, A. Dal Lago, Seismic design and performance of dry-assembled precast structures with adaptable joints. *Soil Dynamics and Earthquake Engineering*, 106, 182-195, 2018.

[22] I. Iervolino, A. Spillatura, P. Bazzurro, RINTC-E project: Towards the assessment of the seismic risk of existing buildings in Italy, RINTC-e: Towards seismic risk assessment of existing residential reinforced concrete buildings in Italy, in *COMPDYN 2019 - 7th ECCOMAS Thematic Conference on Computational Methods in Structural Dynamics and Earthquake Engineering*, Crete, Greece, 2019.

[23] P. Ricci, V. Manfredi, F. Noto, M. Terrenzi, M.T. De Risi, M. Di Domenico, G. Camata, P. Franchin, A. Masi, F. Mollaioli, E. Spacone, G.M. Verderame, RINTC-e: Towards seismic risk assessment of existing residential reinforced concrete buildings in Italy, in *COMPDYN 2019 - 7th ECCOMAS Thematic Conference on Computational Methods in Structural Dynamics and Earthquake Engineering*, Crete, Greece, 2019.

[24] G. Magliulo, D. Bellotti, C. Di Salvatore, F. Cavalieri, RINTC-e project: Towards the seismic risk of low and pre-code single-story r/c precast buildings

in Italy, in *COMPDYN 2019 - 7th ECCOMAS Thematic Conference on Computational Methods in Structural Dynamics and Earthquake Engineering*, Crete, Greece, 2019.

[25] S. Bracchi, S. Cattari, S. Degli Abbati, S. Lagomarsino, G. Magenes, M. Mandirola, S. Marino, A. Penna, M. Rota, RINTC-e project: Towards the seismic risk of retrofitted existing Italian URM buildings, in *COMPDYN 2019 - 7th ECCOMAS Thematic Conference on Computational Methods in Structural Dynamics and Earthquake Engineering*, Crete, Greece, 2019.

[26] G. Cantisani, G. Della Corte, RINTC-e: Seismic risk of pre-code single-story non-residential steel buildings in Italy, in *COMPDYN 2019 - 7th ECCOMAS Thematic Conference on Computational Methods in Structural Dynamics and Earthquake Engineering*, Crete, Greece, 2019.

[27] L. Ragni, D. Cardone, N. Conte, A. Dall'Asta, A. Di Cesare, A. Flora, N. Lamarucciola, F. Micozzi, F. Ponzo, RINTC-e project: the seismic risk of existing Italian RC buildings retrofitted with seismic isolation, in *COMPDYN 2019 - 7th ECCOMAS Thematic Conference on Computational Methods in Structural Dynamics and Earthquake Engineering*, Crete, Greece, 2019.

[28] M. Ercolino, D. Bellotti, G. Magliulo, R. Nascimbene. Vulnerability analysis of industrial RC precast buildings designed according to modern seismic codes. *Engineering Structures*, 158, 67-78, 2018.

[29] D.M. 14/01/2008, Norme Tecniche per le Costruzioni. *Gazzetta Ufficiale della Repubblica Italiana*, 29, 2008.

[30] Circolare n. 617, Istruzioni per l'applicazione delle 'Nuove norme tecniche per le costruzioni' di cui al D.M. 14 gennaio 2008. *Ministero delle infrastrutture e dei trasporti, Gazzetta Ufficiale della Repubblica Italiana*, 47, 2009.

[31] CEN 2004 Eurocode 2, Design of concrete structures - Part 1-1: General rules and rules for buildings. *European Standard*, Brussels, Belgium, 2004.

[32] CEN 2005 Eurocode 3, Design of steel structures - Part 1-8: Design of joints. *European Standard*, Brussels, Belgium, 2005.

[33] CNR 10018, Apparecchi di appoggio per le costruzioni. *Bollettino Ufficiale del CNR*, 1999.

[34] CNR 10025, Istruzioni per il progetto, l'esecuzione ed il controllo delle strutture prefabbricate in calcestruzzo. *Bollettino Ufficiale del CNR*, 1998.

[35] F. McKenna, G.L. Fenves, OpenSees Manual. *Pacific earthquake engineering research cente*r, 2013.

[36] G. Toniolo, B. Dal Lago, Conceptual design and full-scale experimentation of cladding panel connection systems of precast buildings. *Earthquake Engineering and Structural Dynamics*, 46(14), 2565-2586, 2017.

[37] M. Fischinger, M. Kramar, T. Isaković, Cyclic response of slender RC columns typical of precast industrial buildings. *Bulletin of Earthquake Engineering*, 6(3), 519-534, 2008.

[38] A. Belleri, S. Labò, A. Marini, P. Riva, The influence of overhead cranes in the seismic performance of industrial buildings. *Frontiers in Built Environment, section Earthquake Engineering*, 3(64), 2017.

[39] G.D. Kremmyda, Y.M. Fahjan, I.N. Psycharis, S.G. Tsoukantas, Numerical investigation of the resistance of precast RC pinned beam-to-column connections under shear loading. *Earthquake Engineering and Structural Dynamics*, 46, 1511-1529, 2016.

[40] I.N. Psycharis, H.P. Mouzakis, Shear resistance of pinned connections of precast members to monotonic and cyclic loading. *Engineering Structures*, 41, 413–427, 2012.

[41] T.P Tassios, E.N. Vintzeleou, Behavior of dowels under cyclic Deformations. *ACI Structural Journal*, 84 (1), 18-30, 1987.

[42] B. Zoubek, M. Fischinger, T. Isakovic, Estimation of the cyclic capacity of beam-to-column dowel connections in precast industrial buildings. *Bulletin of Earthquake Engineering*, 13(8), 2145-2168, 2015.

[43] G. Magliulo, M. Ercolino, M. Cimmino, V. Capozzi, G. Manfredi, Cyclic shear test on a dowel beam-to-column connection of precast buildings. *Earthquake and Structures*, 9(3), 541-562, 2015.

[44] G. Magliulo, M. Ercolino, M. Cimmino, V. Capozzi, G. Manfredi, FEM analysis of the strength of RC beam-to-column dowel connections under monotonic actions. *Construction and Building Materials*, 69, 271-284, 2014.

[45] EUR 25377 EN, Design guidelines for connections of precast structures under seismic action. *JRC Scientific and Policy Report*, P. Negro and G. Toniolo Eds., 2012.

[46] A. Ferreira, M.K. El Debs, Deformability of beam-column connection with elastomeric cushion and dowel bar to beam axial force. *2nd International Symposium on Prefabrication*, Finland, 2000.

[47] G.D. Kremmyda, Y.M. Fahjan, S.G. Tsoukantas, Nonlinear FE analysis of precast RC pinned beam-to-column connections under monotonic and cyclic shear loading. *Bulletin of Earthquake Engineering*, 2014.

[48] G. Magliulo, D. Bellotti, M. Cimmino, R. Nascimbene, Modeling and seismic response analysis of RC precast Italian code-conforming buildings. *Journal of Earthquake Engineering*; 22(S2), 140-167.